CANCER BIOLOGY & THERAPY
2016, VOL. 17, NO. 12, 1274–1281
http://dx.doi.org/10.1080/15384047.2016.1250986

Taylor & Francis
Taylor & Francis Group

RESEARCH PAPER

OPEN ACCESS

Kmt2a cooperates with menin to suppress tumorigenesis in mouse pancreatic islets

Wenchu Lin[a,b], Joshua M. Francis[b,c], Hong Li[a], Xiaoping Gao[a], Chandra Sekhar Pedamallu[b,c], Patricia Ernst[d], and Matthew Meyerson[b,c]

[a]High Magnetic Field Laboratory, Chinese Academy of Sciences, Hefei, Anhui, P.R. China; [b]Department of Medical Oncology & Center for Cancer Genome Discovery, Dana-Farber Cancer Institute, Harvard Medical School, Boston, MA, USA; [c]Cancer Program, Broad Institute of Harvard and MIT, Cambridge, MA, USA; [d]Department of Pediatrics, The University of Colorado Anschutz Medical Campus, Aurora, USA

ABSTRACT

The reported incidence of pancreatic neuroendocrine tumors (PanNETs) has increased, due in large part to improvements in detection and awareness. However, therapeutic options are limited and a critical need exists for understanding a more thorough characterization of the molecular pathology underlying this disease. The *Men1* knockout mouse model recapitulates the early stage of human PanNET development and can serve as a foundation for the development of advanced mouse models that are necessary for preclinical testing. Menin, the product of the *MEN1* gene, has been shown to physically interact with the KMT2A and KMT2B histone methyltransferases. Both the *KMT2A* and *MEN1* genes are located on chromosome 11q, which frequently undergoes loss of heterozygosity (LOH) in PanNETs. We report herein that inactivation of *Kmt2a* in *Men1*-deficient mice accelerated pancreatic islet tumorigenesis and shortened the average life span. Increases in cell proliferation were observed in mouse pancreatic islet tumors upon inactivation of both *Kmt2a* and *Men1*. The *Kmt2a*/*Men1* double knockout mouse model can be used as a mouse model to study advanced PanNETs.

ARTICLE HISTORY
Received 10 June 2016
Revised 17 September 2016
Accepted 16 October 2016

KEYWORDS
Kmt2a; *Men1*; methyltransferase; PanNETs; tumorigenesis

Introduction

Pancreatic neuroendocrine tumors (PanNETs) arise from the endocrine cells of the pancreas. The World Health Organization (WHO) guidelines grade these tumors as well-differentiated neuroendocrine tumors, well-differentiated neuroendocrine carcinomas and poorly differentiated neuroendocrine carcinomas.[1] Compared to the more common form of pancreatic cancer, adenocarcinoma, which arises in exocrine cells, PanNETs comprise only 2% to 5% of new pancreatic neoplasms according to current diagnostic procedures.[1,2] However, recent epidemiological studies also support that the overall incidence of PanNETs has increased at a statistically significant rate due to improvements in radiological imaging and clinician awareness.[3,4] In addition, the prevalence of PanNETs observed in autopsy studies has been shown to be as high as 10%,[2] suggesting that there may be a great number of undiagnosed, nonfunctional PanNETs in the general population.

The current approach for the treatment of PanNETs is surgical resection and management of hormone hypersecretion if feasible. PanNETs tend to grow at a slower rate and with an overall better prognosis than exocrine tumors.[1] The 5-year survival of PanNETs can be as high as 55% when the tumors are detected before metastasis and are amenable to surgical resection. Once the tumor becomes metastatic, the median overall survival rate is approximately 2 years.[5] The molecular mechanisms underlying this malignancy are poorly understood, and the 5-year survival rate has not significantly improved over the past several decades. The FDA recently approved 2 targeted therapies, sunitinib malate and everolimus, both of which have only shown a modest benefit to patients with PanNETs.[6,7] These shortcomings highlight the need for a better understanding of the molecular pathology of this disease and the urgency of appropriate pre-clinical models to validate potential targets to this type of cancer.

A number of signaling pathways have been shown to be involved in the tumorigenesis of pancreatic neuroendocrine cells such as PI3K signaling, mTOR pathway components and cell cycle regulators. *MEN1* is one of the most commonly mutated genes in PanNETs, with an up to 36% mutation frequency in sporadic localized neuroendocrine tumors and an up to 56% in metastatic neuroendocrine tumors.[8] Recent exon sequencing identified mutations of *ATRX*/*DAXX* both of which are involved in chromatin regulation, providing additional insights into the pathogenesis of PanNETs.[8]

The *Men1* knockout (KO) mouse mimics the phenotypes observed in patients with PanNETs. Studies on the *Men1* KO mouse show that pancreatic neuroendocrine tumors progress though 4 different stages: normal, hyperplasia, atypia and adenoma.[9] In the *Men1* conditional KO mouse model, menin is lost in pancreatic islets during embryogenesis, and hyperplastic islets can be observed as early as

CONTACT Wenchu Lin wenchu@hmfl.ac.cn High Magnetic Field Laboratory, Chinese Academy of Sciences, 350 Shushanhu Rd, Rm 410, Bldg. 2, Hefei, Anhui, China, 230031.

Supplemental data for this article can be accessed on the publisher's website.

2 months. However, frank tumors do not develop until 8 to 10 months of age. In addition, even though hyperplasia is observed in most, if not all of the pancreatic islets, only a small percent of hyperplastic islets ultimately develop tumors. The long tumor latency and sporadic tumor formations in the *Men1* KO mouse model indicate that deletion of *Men1* is sufficient to induce hyperplasia, but that additional somatic events may be required for further tumor progression. LOH analyses also support this notion. Loss of heterozygosity (LOH) analysis on tumors from MEN-1 patients as well as sporadic tumors found that up to 68% of PanNETs exhibit losses of large parts of chromosome 11q.[10]

Kmt2a (*MLL*) encodes a histone H3 lysine 4 specific methyltransferase. It is ubiquitously expressed and plays important roles in many mouse tissues and at different tumor stages.[11-13] Rearrangements of the human *KMT2A* gene by chromosomal translocation are associated with a variety of acute myeloid and lymphoid leukemias.[14] However, the functions of *KMT2A* in solid tumors have not been well characterized. Interestingly, KMT2A is physically associated with menin in conjunction with a number of other proteins to form a COMPASS-like complex that promotes histone H3 methylation.[15] The *KMT2A* gene is located on chromosome segment 11q23 which also frequently undergoes LOH in PanNETs. Based on these observations, we hypothesized that *Kmt2a* might be involved in tumor suppression in pancreatic islet tumors. In this study, we aim to define the role of the TrxG protein Kmt2a in pancreatic islet tumorigenesis using genetically modified mouse models.

Results

Pancreatic islet specific loss of Kmt2a leads to hyperplasia

To address whether *Kmt2a* is required for islet development and homeostasis of adult islets, we crossed the *Kmt2a*$^{f/f}$ mouse with a *RIP-Cre* transgenic mouse to generate *Kmt2a*$^{f/f}$;*RIP-Cre* mice. Immunohistochemical (IHC) analysis for Kmt2a was performed on 2-month old mice to assess Kmt2a protein level changes in mouse pancreatic islets. The results were consistent with *Kmt2a* RT-PCR (Fig. 1A), with Kmt2a being highly expressed (Fig. 1B). However, the Kmt2a protein signal was almost completely lost in *Kmt2a*$^{f/f}$;*RIP-Cre* pancreatic islets upon introduction of *RIP-Cre*(Fig. 1B), suggesting that RIP-Cre could efficiently delete the *Kmt2a* allele in pancreatic islets. Islet-specific *Kmt2a* knockout mice were viable and did not show a reduced lifespan compared to control mice (data not shown). The pancreata from *Kmt2a*$^{f/f}$;*RIP-Cre* mice and control mice were collected at 2 months, 6 months, and 10 months and

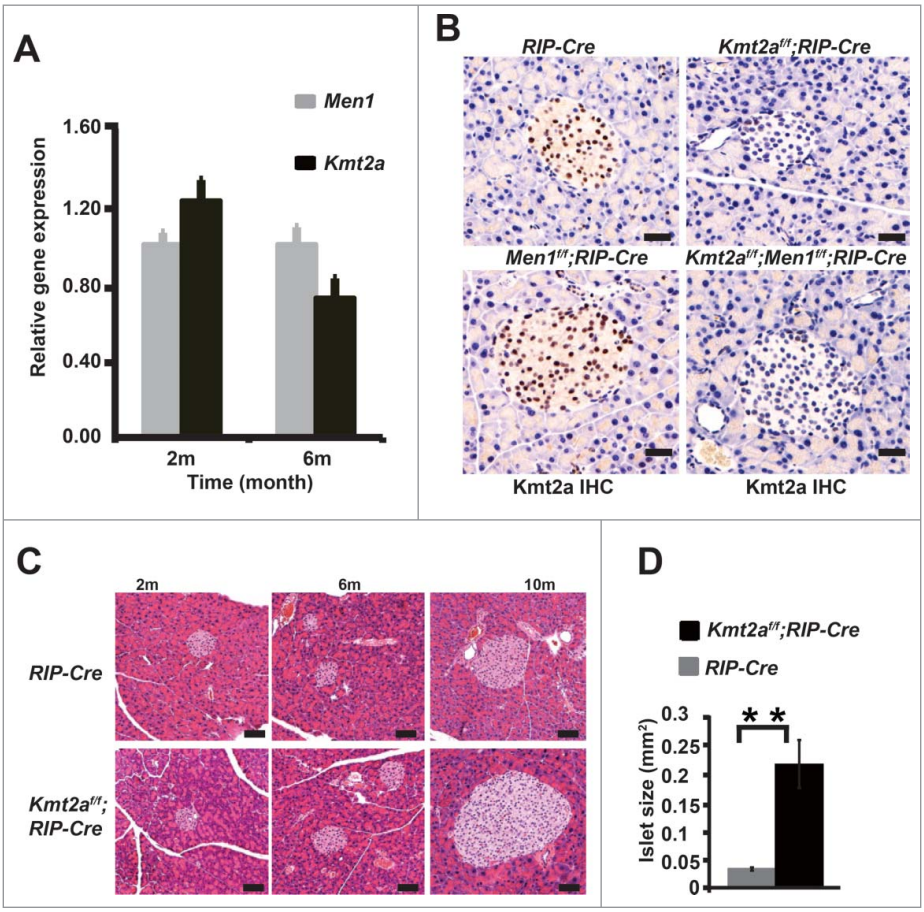

Figure 1. *Kmt2a* inactivation leads to mild islet hyperplasia in mouse pancreatic islets. (A) *Kmt2a* expression was evaluated over time in mouse pancreatic islet cells by RT-PCR. *Men1* expression served as the control. (B) Detection of Kmt2a by immunohistochemistry in *RIP-Cre, Kmt2a*$^{f/f}$;*RIP-Cre, Men1*$^{f/f}$;*RIP-Cre* and *Kmt2a*$^{f/f}$;*Men1*$^{f/f}$;*RIP-Cre* pancreatic islets in 2-month old mice. (C) Representative H&E staining of pancreata from mice with the indicated genotypes. (Scale bar: 100μm) (D) Average pancreatic islet size. Islet size was estimated by measuring the area of an islet using Image J. The 10 largest islets were measured in each mouse, and the average islet size was generated from 80 islets for each genotype.

were examined for islet morphology by histological analysis. At the 2-month stage and 6-month stage, the morphology and size of islets from *Kmt2a*$^{f/f}$;*RIP-Cre* mice were almost indistinguishable from those in control mice, indicating that *Kmt2a* is not required for pancreatic islet development. However, at 10-months the islets in *Kmt2a*$^{f/f}$;*RIP-Cre* mice were significantly larger than those in control mice, suggesting that *Kmt2a* inactivation causes a hyperplastic phenotype (Figs. 1C and 1D). Further analysis of *Kmt2a*$^{f/f}$;*RIP-Cre* mice at 12 months and 16 months confirmed the presence of hyperplasia, but no frank tumors were detected in *Kmt2a*$^{f/f}$;*RIP-Cre* mice (data not shown). This study indicates that ablation of *Kmt2a* can cause modest hyperplasia in mouse pancreatic islets even though *Kmt2a* loss does not lead to pancreatic islet tumors on its own.

Ablation of Kmt2a in the Men1-deficient mouse leads to reduced survival through hyperinsulinemia and hypoglycemia

To address whether *Kmt2a* inactivation has biological consequences in mice with a *Men1* null background, we generated *Kmt2a*$^{f/f}$;*Men1*$^{f/f}$;*RIP-Cre* mice. Kmt2a IHC on islets from *Kmt2a*$^{f/f}$;*Men1*$^{f/f}$;*RIP-Cre* mice showed that the Kmt2a signal is almost completely lost (Fig. 1B). Over time, the median survival time for *Men1*$^{f/f}$;*RIP-Cre* mice (N = 25) was 313 days, while the median survival time for *Kmt2a*$^{f/f}$;*Men1*$^{f/f}$;*RIP-Cre* mice (N = 16)was markedly shorter at 258 days, indicating that *Kmt2a* loss shortens the life span of *Men1*-deficient mice (Fig. 2A). Similarly, within the same littermates the median survival time for *Kmt2a*$^{f/f}$;*Men1*$^{f/f}$;*RIP-Cre* mice (N = 10) was 274 d compared to 334 d for *Men1*$^{f/f}$;*RIP-Cre* mice (N = 12) when both *Kmt2a*$^{f/f}$;*Men1*$^{f/f}$;*RIP-Cre* mice and *Men1*$^{f/f}$;*RIP-Cre* mice were generated from the same littermates (Fig. S1).

The plasma insulin levels were measured at 2 months, 4 months, 6 months, 8 months and 10 months to assess hypoglycemia within the cohort. In *Men1*$^{f/f}$;*RIP-Cre* mice the plasma insulin levels began to gradually increase at ~4 months of age and became significantly elevated by 6 months, whereas the plasma insulin levels in *Kmt2a*$^{f/f}$;*Men1*$^{f/f}$;*RIP-Cre* mice began to rise at 4 months and then quickly surpassed *Men1*$^{f/f}$;*RIP-Cre* mouse insulin levels (Fig. 2B). These results suggest that the combined loss of kmt2a and Men1 leads to an earlier onset of tumor formation as evidenced by hyperinsulinemia.

Ablation of Kmt2a promotes tumorigenesis in Men1-deficient pancreatic islets

We harvested mouse pancreata from *Men1*$^{f/f}$;*RIP-Cre* and from *Kmt2a*$^{f/f}$;*Men1*$^{f/f}$;*RIP-Cre* mice and conducted histological analysis to examine pancreatic islet size. We found that the islet cell morphology and islet size in *Kmt2a*$^{f/f}$;*Men1*$^{f/f}$;*RIP-Cre* mice were indistinguishable from that in *Men1*$^{f/f}$;*RIP-Cre* mice at age of 2 months and 4 months (Fig. 3A). However, by 6 months of age, the islets in *Kmt2a*$^{f/f}$;*Men1*$^{f/f}$;*RIP-Cre* mice were larger than those in *Men1*$^{f/f}$;*RIP-Cre* mice. When the pancreas was harvested from both strains at the 10-month stage, the islet tumor size and the islet cell morphology in *Kmt2a*$^{f/f}$;*Men1*$^{f/f}$;*RIP-Cre* mice were consistently different from that in the *Men1*$^{f/f}$;*RIP-Cre* mice (Fig. 3A). The average islet tumor size was 2 times larger in *Kmt2a*$^{f/f}$;*Men1*$^{f/f}$;*RIP-Cre* mice than in *Men1*$^{f/f}$;*RIP-Cre* mice (Fig. 3B). Additionally, the size of both the nucleus and cytoplasm were larger in the *Kmt2a*$^{f/f}$;*Men1*$^{f/f}$;*RIP-Cre* mice than that in *Men1*$^{f/f}$;*RIP-Cre* mice (Fig. 3A).We also observed that there were a greater number of tumors detected in the *Kmt2a*$^{f/f}$;*Men1*$^{f/f}$;*RIP-Cre* mice than that in *Men1*$^{f/f}$;*RIP-Cre* mice. When we defined abnormal islets as being larger than 0.5 mm with showing strong vascularization, we found 5 tumors in *Kmt2a*$^{f/f}$;*Men1*$^{f/f}$;*RIP-Cre* mice on average compared to only 1.3 tumors on average in *Men1*$^{f/f}$;*RIP-Cre* mice (Fig. 3C).In general, the tumor phenotypes in *Kmt2a*$^{f/f}$;*Men1*$^{f/f}$;*RIP-Cre* mice were more advanced than the tumors in *Men1*$^{f/f}$;*RIP-Cre* mice (Table S1). Thus, inactivation of *Kmt2a* in pancreatic islets promotes tumor progression rather than facilitating tumor initiation. We also observed that there were more blood vessels in tumors from the *Kmt2a*$^{f/f}$;*Men1*$^{f/f}$;*RIP-Cre* mice compared to *Men1*$^{f/f}$;*RIP-Cre* mice (Figs. S2A and S2B).

Kmt2a loss results in more cell proliferation in hyperplastic islets and tumors in Kmt2a$^{f/f}$; Men1$^{f/f}$; RIP-Cre mice

We next utilized immunohistochemical analysis to investigate whether the larger hyperplastic islets and increased number of tumors observed in *Kmt2a*$^{f/f}$;*Men1*$^{f/f}$;*RIP-Cre* mice were a consequence of increased cell proliferation or reduced apoptosis. We found that there were elevated numbers of mitotic cells in

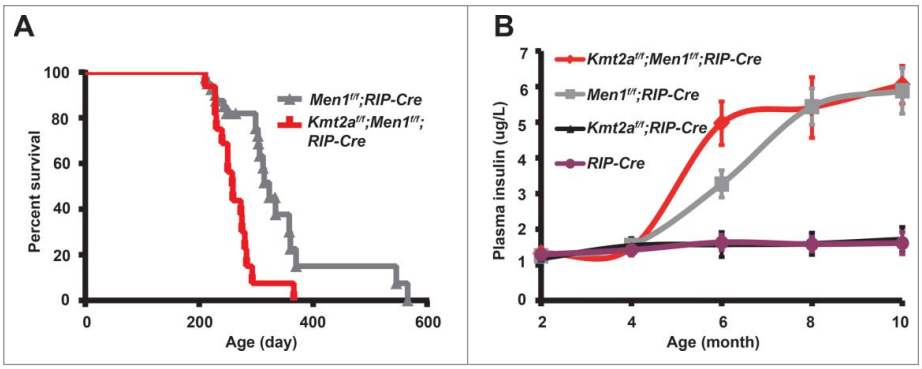

Figure 2. Loss of *Kmt2a* shortens life span in *Men1*-deficient mice. (A) Kaplan-Meier survival curves comparing *Men1*$^{f/f}$;*RIP-Cre* mice (n = 24) with *Kmt2a*$^{f/f}$; *Men1*$^{f/f}$;*RIP-Cre* mice (n = 16; P < 0.0001). (B) Circulating insulin levels in mice with the indicated genotypes (paired sample t test: p = 0.03 at 6 months).

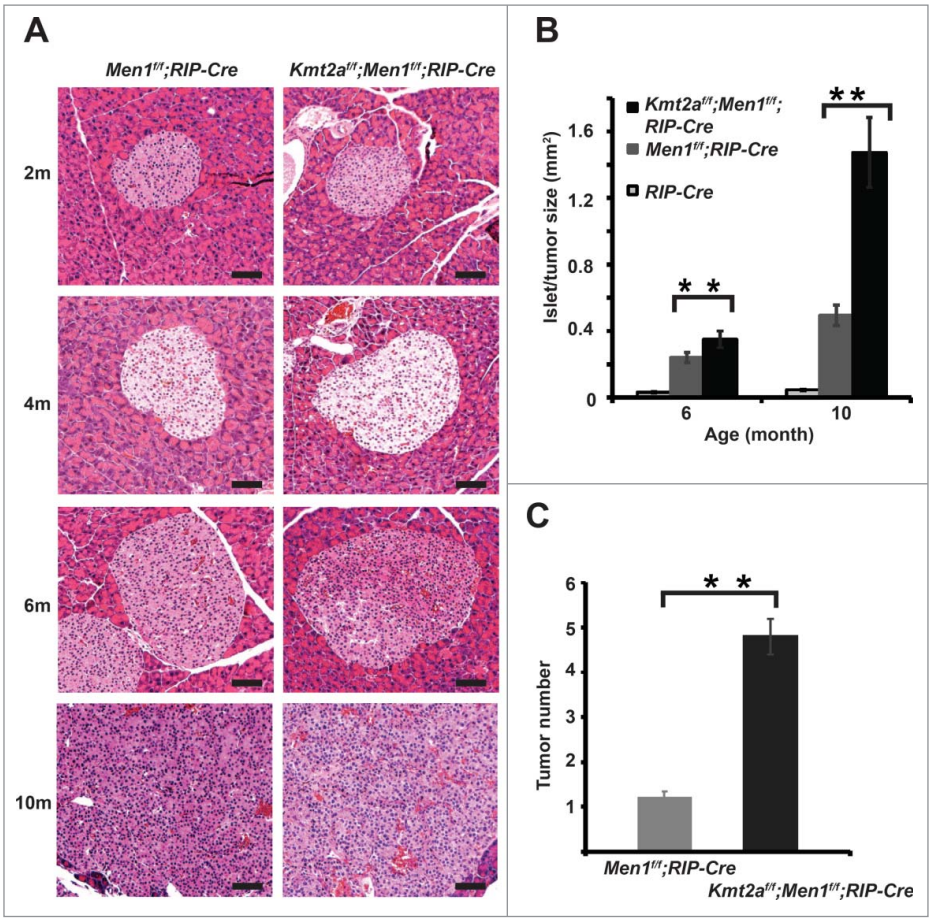

Figure 3. Ablation of *Kmt2a* accelerates *Men1*-defective pancreatic islet cell tumorigenesis. (A) Representative H&E staining of pancreata from mice with the indicated genotypes. (Scale bar: 100μm) (B) Average pancreatic islet/tumor size. Islet size was estimated by measuring the islet area (tumor in *Men1*$^{f/f}$;*RIP-Cre* mice and *Kmt2a*$^{f/f}$;*Men1*$^{f/f}$;*RIP-Cre* mice) using Image J. The 10 largest islets were measured in each mouse and the average islet size was generated from 100 islets for each genotype. (C) Average tumor numbers in *Men1*$^{f/f}$;*RIP-Cre* mice and *Kmt2a*$^{f/f}$;*Men1*$^{f/f}$;*RIP-Cre* mice.

Kmt2a$^{f/f}$;*Men1*$^{f/f}$;*RIP-Cre* mice compared to *Men1*$^{f/f}$;*RIP-Cre* mice (Figs. 4A and 4B). A PanNET is considered to be a malignant tumor if there are more than 20 mitotic cells in 10 high power fields.[16] There were approximately 20 more mitotic cells in one *Kmt2a*$^{f/f}$;*Men1*$^{f/f}$;*RIP-Cre* tumor than that in a comparable the *Men1*$^{f/f}$;*RIP-Cre* tumor(Fig. 4C), indicating that tumors caused by *Men1* and *Kmt2a* loss are more proliferative than those caused by loss of *Men1* alone.

Next we performed IHC staining for the mitotic marker H3S10P[17]in islets harvested from *RIP-Cre, Men1*$^{f/f}$;*RIP-Cre* and *Kmt2a*$^{f/f}$;*Men1*$^{f/f}$;*RIP-Cre* mice. As expected, the *Men1*$^{f/f}$;*RIP-Cre* islets showed more H3S10P positive cells than *RIP-Cre* control islets (Fig. 5A). However, In *Kmt2a*$^{f/f}$;*Men1*$^{f/f}$;*RIP-Cre* islets, there were many more H3S10P positive cells when compared with *Men1*$^{f/f}$;*RIP-Cre* islets, thus demonstrating increased mitosis(Fig. 5A). Quantification of H3S10P positive cells showed that there were 8 times more mitotic cells in *Kmt2a*$^{f/f}$;*Men1*$^{f/f}$;*RIP-Cre* islets than that in *Men1*$^{f/f}$;*RIP-Cre* islets (Fig. 5C). Additionally, H3S10P staining in 10-month islets/tumors consistently showed more H3S10P positive cells in *Kmt2a*$^{f/f}$;*Men1*$^{f/f}$;*RIP-Cre* tumors compared to that in *Men1*$^{f/f}$;*RIP-Cre* tumors (Figs. S3A and S3C).

TUNEL assays performed on islets/tumors from *RIP-Cre, Men1*$^{f/f}$;*RIP-Cre* and *Kmt2a*$^{f/f}$;*Men1*$^{f/f}$;*RIP-Cre* mice revealed that there were similar numbers of apoptotic cells in all 3 of the tested trains (Figs. 5B and 5D). Cleaved Caspase-3 (CC3) IHC staining was also performed in these islets; similar numbers of CC3 positive cells were observed in the islets (Figs. S3B and S3D). Statistical analyses did not show a significant difference between islets. These studies indicate that the more highly mitotic tumor phenotypes observed in *Kmt2a*$^{f/f}$;*Men1*$^{f/f}$; *RIP-Cre* mice were more likely due to increased cell proliferation rather than decreased apoptosis.

Discussion

Kmt2a function during islet development and islet function in the adult stage

Kmt2a functions are not only critical for embryonic development, but are also essential for the maintenance of homeostasis in particular lineage/tissues such as haematopoietic stem cells as well as during neurogenesis in mouse postnatal brain.[13] *Kmt2a* is also highly expressed in mouse pancreatic islets. Our study reveals that *Kmt2a* is dispensable for islet development as there is no detectable difference in islet numbers in *Kmt2a*-deficient mice compared with *RIP-Cre* control mice. However, *Kmt2a* is required for adult islet homeostasis as the loss of *Kmt2a* was found to lead to advanced hyperplasia in adult mice. Our

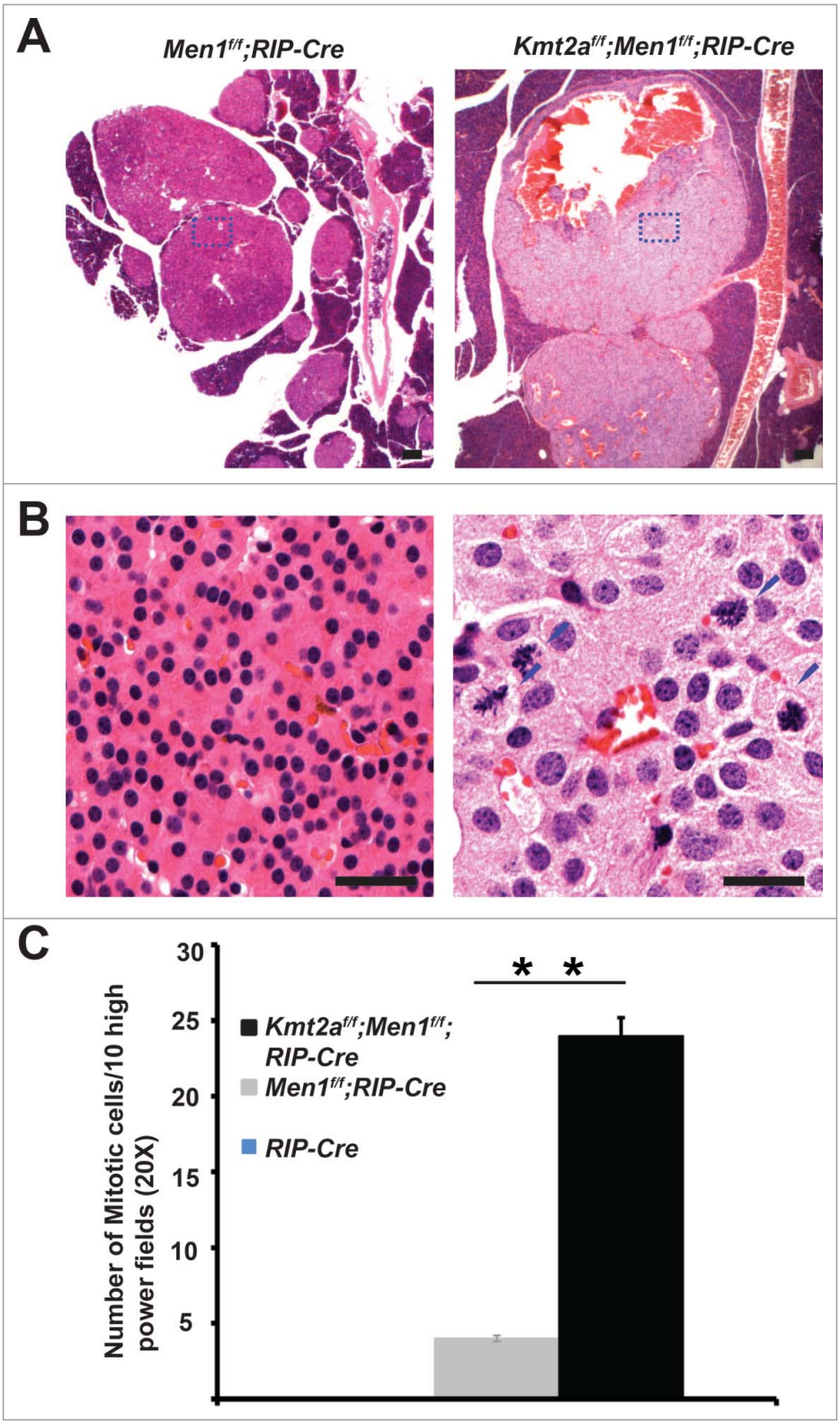

Figure 4. *Kmt2a* loss leads to a robust increase in mitotic cells. Mitotic cells were observed from *Kmt2a*$^{f/f}$;*Men1*$^{f/f}$;*RIP-Cre* but not in *Men1*$^{f/f}$;*RIP-Cre* islets in (A) (lower magnification, Scale bar: 100 μm) and (B) (higher magnification, Scale bar: 100μm). Arrow indicates cells undergoing mitosis.(C): Quantification of mitotic cells from hyperplastic islets/tumors harvested from mice with the indicated genotypes at an age of 10 months.

investigation indicates that *Kmt2a* is not a neuroendocrine-specific tumor suppressor as no tumors were observed in *Kmt2a*-deficient mice. Consistent with this observation, we did not observe any survival disadvantage upon *Kmt2a* loss in islets. Possible explanations include: *Kmt2a* function might indeed be dispensable for islet cell differentiation and/or *Kmt2a* loss might be compensated by *Kmt2a* family members such as *Kmt2b, Kmt2c*, or *Kmt2d*.

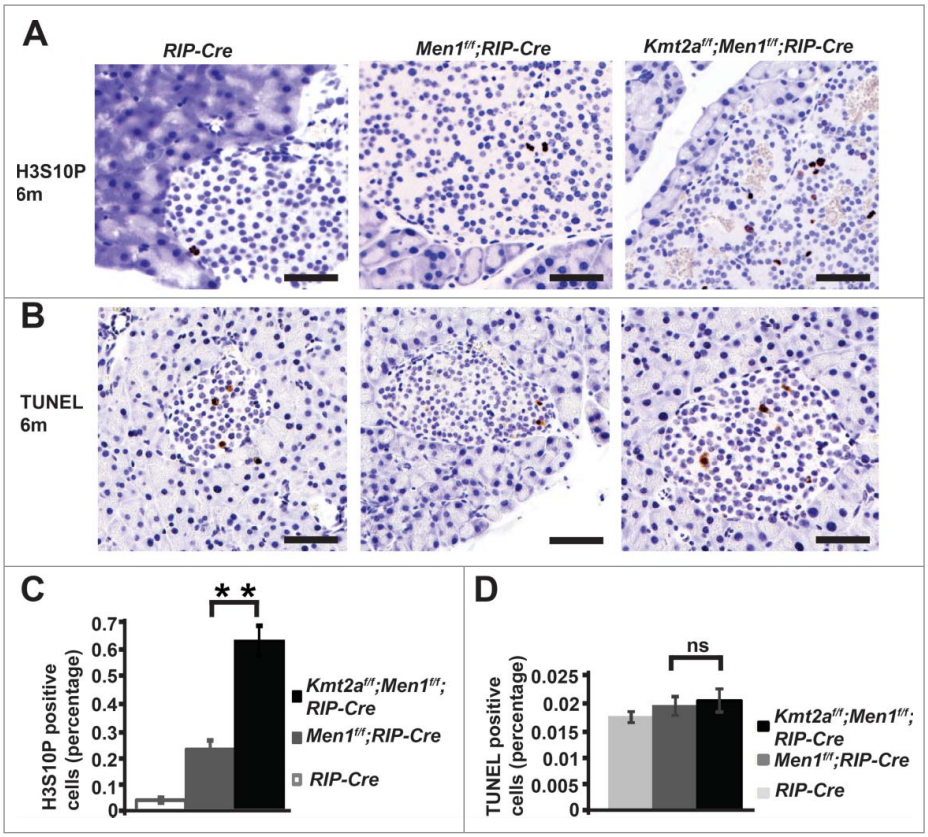

Figure 5. More cell proliferation rather than less apoptosis is observed in *Kmt2a*$^{f/f}$;*Men1*$^{f/f}$;*RIP-Cre* islets in 6-month old mice. (A) Histone H3 serine 10 phosphorylation was evaluated in pancreatic islet cells at the age of 6 months with the indicated genotypes by immunohistochemistry (IHC). The dark brown color indicates positivity for Anti-Histone H3(phospho S10). (B) Apoptosis was measured via TUNEL assay. The dark brown color indicates apoptosis positive cells. (C) Quantification of proliferating cells from hyperplastic islets harvested from mice with the indicated genotypes at an age of 6 months. **, $P < 0.01$ (D) Quantification of apoptotic cells from hyperplastic islets harvested from mice with the indicated genotypes at an age of 6 months.

Kmt2a cooperates with MEN1 *to prevent tumor formation*

Men1-deficent islets quickly become hyperplastic at 2 to 4 months of age. However, it takes 6 to 8 months for the hyperplastic islet to develop detectable tumors. Thus, other genetic or epigenetic alterations must likely occur to facilitate tumor progression. During human MEN-1 syndrome, *MEN1* is mutated at the germline level and the second allele is frequently lost through LOH, which often involves a broad region of 11q. As *KMT2A* is located in 11q23 within 10 Mb of the *MEN1* locus, *KMT2A* is frequently lost in tumors from patients with MEN-1 syndrome. Although *Kmt2a* loss in mice by itself does not lead to tumor formation, *Kmt2a* inactivation accelerates islet tumor progression in the *Men1*-deficient mouse. This study indicates that *Men1* is a driver and initiator of islet tumors whereas *Kmt2a* loss can facilitate tumor progression. Kmt2a might be involved in islet tumorigenesis in both a menin-dependent and a menin-independent manner. As a menin-associated protein, Kmt2a might partially compensate for menin dysfunction and maintain key downstream targets. Whereas when Kmt2a is inactivated, menin might counteract the effect caused by Kmt2a loss. On the other hand, although menin is a component of the COMPASS-like complex that promotes histone H3 methylation under certain circumstance, Kmt2a might be critical for certain important genes in pancreatic islets which are independent of menin. Our preliminary ChIP-seq and RNA-Seq data (unpublished) show that the expression of several islet-specific transcription factors is positively regulated by Kmt2a enzymatic activity, but not menin activity. Further experiments should be conducted to address these remaining questions.

Advanced mouse models for molecular pathology studies and preclinical studies

Currently two targeted therapies for pancreatic neuroendocrine tumors have been approved by the FDA,[6,7] indicating that targeted therapies can be developed for the treatment of pancreatic neuroendocrine cancer. However, current targeted therapies only prolong progression-free survival for approximately 6 months,[6,7] providing only a modest benefit to patients with this type of cancer. Additionally the response rates are very low when patients with advanced PanNETs were treated with the tyrosine kinase inhibitor sunitinib and the mTOR inhibitor everolimus.[6,7] Targeted therapeutic approaches which combine the effect of both mTOR inhibition and angiogenesis inhibition have shown substantial anti-cancer activity,[18] and new potential approaches have been proposed.[2] In principle, better mouse models will help to develop improved targeted therapies. The *Kmt2a*$^{f/f}$;*Men1*$^{f/f}$;*RIP-Cre* mouse has more advanced tumor phenotypes than other models, so this mouse model may be more suitable as a preclinical mouse model for testing new targeted therapies for pancreatic neuroendocrine

tumors. In addition, menin is physically associated with Kmt2a, which is critical in leukemia mediated by Kmt2a fusion proteins. Several inhibitors that specifically disrupted the menin-Kmt2a interaction have been developed and pharmacologic inhibition has shown a very promising response.[19-21] Disruption of *Kmt2a* does not lead to phenotypes in early stage of islets whereas *Men1* deletion causes a hyperplastic phenotype, suggesting that menin has Kmt2a-independent roles in the maintenance of homeostasis in mouse pancreatic islets, which is consistent with a recent study in the haematopoietic system.[22] This observation may alleviate some concern regarding the potential strong side effect on pancreatic function when applying these MI-2 and related inhibitors in patients with *Kmt2a*-associated leukemia.

Materials and methods

Generation of mouse strains

The creation and genotyping of *RIP-Cre* mice, *Men1*^{flf};*RIP-Cre* mice has been described previously.[23] *Kmt2a*^{flf} mice were crossed with *RIP-Cre* mice[24] to obtain *Kmt2a*$^{f/+}$;*RIP-Cre* mice. *Kmt2a*$^{f/+}$;*RIP-Cre* mice were crossed with *Kmt2a*$^{f/+}$mice to generate *Kmt2a*$^{f/f}$;*RIP-Cre* mice. *Kmt2a*$^{f/f}$ mice were crossed with *Men1*^{flf};*RIP-Cre* mice to obtain *Kmt2a*$^{f/+}$;*Men1*$^{fl+}$;*RIP-Cre, Kmt2a*$^{f/+}$;*Men1*$^{fl+}$;*RIP-Cre* were then crossed with *Kmt2a*$^{f/+}$;*Men1*$^{fl+}$ mice to obtain *Kmt2a*$^{f/f}$;*Men1*^{flf};*RIP-Cre* mice. Mice were maintained on a mixed 129s6, FVB/N, and C57BL/6 background. All mice were maintained in the research animal facility of the Dana–Farber Cancer Institute and Hefei Institutes of Physical Science Laboratory Animal Center, Chinese Academy of Sciences. All procedures were performed in accordance with the National Research Council Guide for the Care and Use of laboratory Animals and were approved by the Institutional Animal Care and Use Committee of both the Dana-Farber Cancer Institute and Hefei Institutes of Physical Science, Chinese Academy of Sciences.

Isolation of mouse pancreatic islets

Pancreatic islets were isolated as previously described.[23]

Circulating insulin measurement

Blood was collected via the submandibular vein method after the mice were fasted for 16h. Plasma was prepared by spinning a tube of fresh blood containing an anticoagulant. The circulating insulin level was measured using an ultra sensitive Mouse ELISA kit (Crystal Chemical, Downers Grove, IL, USA) according to the manufacturer's instructions.

Histological and immunohistochemical analysis of pancreatic tissues

Pancreata were collected from mice at indicated time points and fixed in 4% paraformaldehyde for 2 hours followed by dehydration and paraffin embedding. Histopathological analysis was carried out on 5-micrometer sections stained with hematoxylin and eosin. Islet morphology and tumors were examined in at least 3 cut sections for each pancreas after staining with hematoxylin and eosin. Appropriate positive and negative controls were run on matched sections for all applied antibodies. Immunohistochemical staining was performed on serial sections using antibodies against *Kmt2a* (GeneTax, GTX17959, 1:400), Anti-Histone H3(Phospho S10) (Abcam, Ab14955, 1:180), and CC3 (Thermo, PA1-24473. 1:100). Sections were counterstained in Meyer's hematoxylin, mounted and photographed using an Olympus microscope.

RNA isolation and RT-qPCR

Total RNA was extracted using the RNeasy kit (Qiagen) from 100 to 300 mouse pancreatic islets purified from 2 mice with different genotypes according to the manufacturer's instructions. For RT-PCR, DNase I (Qiagen)-treated RNA samples were reverse transcribed using oligo-dT and SuperScript III (Invitrogen), with first strand cDNA for PCR created using SYBR green PCR mix (Qiagen, Valencia, California, United States) in an Applied Biosystems 7300 Real Time-PCR system (Foster City, California, United States). PCR primer pairs were designed to amplify 150- to 200-bp fragments from select genomic regions. Quantification of mRNA expression in each sample was performed by normalizing values to the expression values for *Gapdh*. Primer sequences for *Kmt2a* are 5′-CATTCGGCAAATGGAGCGAG-3′(forward) and 5′-TAGAGGAGGCTGCTCAGT GT-3′ (reverse); primer sequences for *Men1* are 5′-GATGGACATCTCTGAGACCCA-3′(forward) and 5′-CCAGTCCCTCTTCAGCTTCA-3′(reverse); primer sequences for *Gapdh* are 5′-TCAATGAAGGGGTCGTTGAT-3′ (forward) and 5′-CGTCCCGTAGACAAAATGGT-3′ (reverse).

Disclosure of potential conflicts of interest

No potential conflicts of interest were disclosed.

Acknowledgments

We thank members of the Meyerson laboratory and members of the Lin laboratory for critical reading of the manuscript and helpful discussions, the Harvard Specialized Histopathology Services-Longwood for histology, and the Joslin Diabetes Center Core facility for islet isolation.

References

1. Halfdanarson TR, Rubin J, Farnell MB, Grant CS, Petersen GM. Pancreatic endocrine neoplasms: epidemiology and prognosis of pancreatic endocrine tumors. Endocrine-related Cancer 2008; 15:409-27; PMID:18508996; http://dx.doi.org/10.1677/ERC-07-0221
2. Zhang J, Francois R, Iyer R, Seshadri M, Zajac-Kaye M, Hochwald SN. Current understanding of the molecular biology of pancreatic neuroendocrine tumors. J Natl Cancer Inst 2013; 105:1005-17; PMID:23840053; http://dx.doi.org/10.1093/jnci/djt135
3. Yao JC, Hassan M, Phan A, Dagohoy C, Leary C, Mares JE, Abdalla EK, Fleming JB, Vauthey JN, Rashid A, et al. One hundred years after "carcinoid": epidemiology of and prognostic factors for neuroendocrine tumors in 35,825 cases in the United States. J Clin Oncol 2008; 26:3063-72; PMID:18565894; http://dx.doi.org/10.1200/JCO.2007.15.4377
4. Franko J, Feng W, Yip L, Genovese E, Moser AJ. Non-functional neuroendocrine carcinoma of the pancreas: incidence, tumor biology, and outcomes in 2,158 patients. J Gastrointest Surg 2010; 14:541-8; PMID:19997980; http://dx.doi.org/10.1007/s11605-009-1115-0
5. Hill JS, McPhee JT, McDade TP, Zhou Z, Sullivan ME, Whalen GF, Tseng JF. Pancreatic neuroendocrine tumors: the impact of surgical

resection on survival. Cancer 2009; 115:741-51; PMID:19130464; http://dx.doi.org/10.1002/cncr.24065
6. Raymond E, Dahan L, Raoul JL, Bang YJ, Borbath I, Lombard-Bohas C, Valle J, Metrakos P, Smith D, Vinik A, et al. Sunitinib malate for the treatment of pancreatic neuroendocrine tumors. N Engl J Med 2011; 364:501-13; PMID:21306237; http://dx.doi.org/10.1056/NEJMoa1003825
7. Yao JC, Shah MH, Ito T, Bohas CL, Wolin EM, Van Cutsem E, Hobday TJ, Okusaka T, Capdevila J, de Vries EG, et al. Everolimus for advanced pancreatic neuroendocrine tumors. N Engl J Med 2011; 364:514-23; PMID:21306238; http://dx.doi.org/10.1056/NEJMoa1009290
8. Jiao Y, Shi C, Edil BH, de Wilde RF, Klimstra DS, Maitra A, Schulick RD, Tang LH, Wolfgang CL, Choti MA, et al. DAXX/ATRX, MEN1, and mTOR pathway genes are frequently altered in pancreatic neuroendocrine tumors. Science 331:1199-203; PMID:21252315; http://dx.doi.org/10.1126/science.1200609
9. Crabtree JS, Scacheri PC, Ward JM, McNally SR, Swain GP, Montagna C, Hager JH, Hanahan D, Edlund H, Magnuson MA, et al. Of mice and MEN1: Insulinomas in a conditional mouse knockout. Mol Cell Biol 2003; 23:6075-85; PMID:12917331; http://dx.doi.org/10.1128/MCB.23.17.6075-6085.2003
10. Duerr EM, Chung DC. Molecular genetics of neuroendocrine tumors. Best Pract Res Clin Endocrinol Metab 2007; 21:1-14; PMID:17382262; http://dx.doi.org/10.1016/j.beem.2006.12.001
11. Yu BD, Hess JL, Horning SE, Brown GA, Korsmeyer SJ. Altered Hox expression and segmental identity in Mll-mutant mice. Nature 1995; 378:505-8; PMID:7477409; http://dx.doi.org/10.1038/378505a0
12. Jude CD, Climer L, Xu D, Artinger E, Fisher JK, Ernst P. Unique and independent roles for MLL in adult hematopoietic stem cells and progenitors. Cell Stem Cell 2007; 1:324-37; PMID:18371366; http://dx.doi.org/10.1016/j.stem.2007.05.019
13. Lim DA, Huang YC, Swigut T, Mirick AL, Garcia-Verdugo JM, Wysocka J, Ernst P, Alvarez-Buylla A. Chromatin remodelling factor Mll1 is essential for neurogenesis from postnatal neural stem cells. Nature 2009; 458:529-U9; PMID:19212323; http://dx.doi.org/10.1038/nature07726
14. Muntean AG, Hess JL. The pathogenesis of mixed-lineage leukemia. Ann Rev Pathol 2012; 7:283-301; PMID:22017583; http://dx.doi.org/10.1146/annurev-pathol-011811-132434
15. Eissenberg JC, Shilatifard A. Histone H3 lysine 4 (H3K4) methylation in development and differentiation. Dev Biol 2010; 339:240-9; PMID:19703438; http://dx.doi.org/10.1016/j.ydbio.2009.08.017
16. Chen M, Van Ness M, Guo Y, Gregg J. Molecular pathology of pancreatic neuroendocrine tumors. J Gastrointestinal Oncol 2012; 3:182-8; PMID:22943010; http://dx.doi.org/10.3978/j.issn.2078-6891.2012.018
17. Hendzel MJ, Wei Y, Mancini MA, Van Hooser A, Ranalli T, Brinkley BR, Bazett-Jones DP, Allis CD. Mitosis-specific phosphorylation of histone H3 initiates primarily within pericentromeric heterochromatin during G2 and spreads in an ordered fashion coincident with mitotic chromosome condensation. Chromosoma 1997; 106:348-60; PMID:9362543; http://dx.doi.org/10.1007/s004120050256
18. Hobday TJ, Qin R, Reidy-Lagunes D, Moore MJ, Strosberg J, Kaubisch A, Shah M, Kindler HL, Lenz HJ, Chen H, et al. Multicenter Phase II Trial of Temsirolimus and Bevacizumab in Pancreatic Neuroendocrine Tumors. J Clin Oncol 2015; 33:1551-6; PMID:25488966; http://dx.doi.org/10.1200/JCO.2014.56.2082
19. Grembecka J, He S, Shi A, Purohit T, Muntean AG, Sorenson RJ, Showalter HD, Murai MJ, Belcher AM, Hartley T, et al. Menin-MLL inhibitors reverse oncogenic activity of MLL fusion proteins in leukemia. Nat Chem Biol 2012; 8:277-84; PMID:22286128; http://dx.doi.org/10.1038/nchembio.773
20. Zhou H, Liu L, Huang J, Bernard D, Karatas H, Navarro A, Lei M, Wang S. Structure-based design of high-affinity macrocyclic peptidomimetics to block the menin-mixed lineage leukemia 1 (MLL1) protein-protein interaction. J Med Chem 2013; 56:1113-23; PMID:23244744; http://dx.doi.org/10.1021/jm3015298
21. Borkin D, He S, Miao H, Kempinska K, Pollock J, Chase J, Purohit T, Malik B, Zhao T, Wang J, et al. Pharmacologic inhibition of the Menin-MLL interaction blocks progression of MLL leukemia in vivo. Cancer Cell 2015; 27:589-602; PMID:25817203; http://dx.doi.org/10.1016/j.ccell.2015.02.016
22. Li BE, Gan T, Meyerson M, Rabbitts TH, Ernst P. Distinct pathways regulated by menin and by MLL1 in hematopoietic stem cells and developing B cells. Blood 2013; 122:2039-46; PMID:23908472; http://dx.doi.org/10.1182/blood-2013-03-486647
23. Lin W, Cao J, Liu J, Beshiri ML, Fujiwara Y, Francis J, Cherniack AD, Geisen C, Blair LP, Zou MR, et al. Loss of the retinoblastoma binding protein 2 (RBP2) histone demethylase suppresses tumorigenesis in mice lacking Rb1 or Men1. Proc Natl Acad Sci U S A; 108:13379-86; PMID:21788502; http://dx.doi.org/10.1073/pnas.1110104108
24. Herrera PL. Adult insulin- and glucagon-producing cells differentiate from two independent cell lineages. Development 2000; 127:2317-22; PMID:10804174